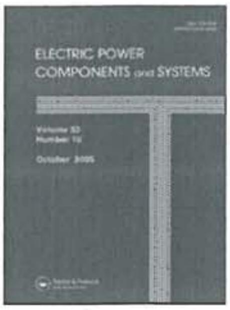

Taylor & Francis
Taylor & Francis Group

Electric Power Components and Systems

ISSN: 1532-5008 (Print) 1532-5016 (Online) Journal homepage: http://www.tandfonline.com/loi/uemp20

Multi-Agent Based Distributed Voltage Control Algorithm for Smart Grid Applications

Patrick T. Manditereza & Ramesh C. Bansal

Electric Power Components and Systems, 44(20):2352–2363, 2016

ISSN: 1532-5008 print / 1532-5016 online
DOI: 10.1080/15325008.2016.1219889

Multi-Agent Based Distributed Voltage Control Algorithm for Smart Grid Applications

Patrick T. Manditereza[1] and Ramesh C. Bansal[2]
[1]Department of Electrical, Electronic, and Computer Engineering, Central University of Technology, Free State, South Africa
[2]Department of Electrical, Electronic, and Computer Engineering, University of Pretoria, South Africa

CONTENTS

Abstract—The integration of renewable energy generators in distribution networks has increased the complexity of the voltage control problem rendering traditional control methods ineffective. This article proposes a voltage control algorithm for radial distribution systems, based on multi-agent systems, that eliminates any voltage deviation resulting from connection of distributed generators or variation of loading conditions. To realize distributed control, the distribution feeder is split into a series of overlapping segments. An agent is allocated to each segment and senses the voltage variables in its segment. The overlapping feature is realized through the exchange of information between an agent and the agents in the two adjacent segments. The agent in a segment then formulates reactive power compensation sufficient to restore the voltage in that segment. The total coordinated actions of the agents eliminate any voltage deviations, restoring the feeder voltage profile to the pre-planned base case profile. The main advantage of the proposed approach is that the agents can solve the voltage problem without the intervention of any central controller and by communicating only with its immediate neighbors. The results of case studies show that the proposed method is effective in controlling the voltage profile of a distributed generator-integrated distribution system.

1. INTRODUCTION

The concept of the smart grid brings new challenges to distribution system voltage control. The integration of renewable energy generators in smart grids, such as wind and solar photovoltaic (PV) generators, which are dispersed according to resource availability has increased the complexity of the voltage control problem [1]. Distributed generator (DG) connection causes reduction in the current flow from the upstream substation, and may additionally, depending on the operating mode, inject (export) vars, or consume (import) vars. The net effect is the raising or lowering of the distribution network voltage profile depending on the type of DG that is connected. This problem tends to be serious in distribution systems whose configuration is radial with low X/R ratio [2, 3].

Conventional voltage regulation equipment may be confused by the connection of DG. On-load-tap changer (OLTC)

Keywords: distributed generation, voltage control, sensitive-based voltage control, multi-agent systems, distributed control, DG integration, smart grid, sensitivity coefficients, Jacobian matrix, reactive power dispatch
Received 9 February 2016; accepted 23 July 2016
Address correspondence to Ramesh C. Bansal, Department of Electrical, Electronic, and Computer Engineering, University of Pretoria, Pretoria-0028, South Africa. E-mail: rcbansal@ieee.org
Color versions of one or more of the figures in the article can be found online at www.tandfonline.com/uemp.

control within the substation is only able to regulate the voltage at the substation, and the voltage profile downstream may remain uncontrolled and can deviate outside of the accepted range. Similarly, voltage compensation from a line-drop-compensator (LDC) is reduced since the DG decreases the load observed at the LDC control, leaving the downstream voltage profile uncertain and dependent on the DG type. Basically, these local controllers are not able to control the voltage profile of a DG-integrated distribution system. Distributed components, such as voltage regulators (VRs), shunt capacitor banks, and static compensators, can be placed at points along the distribution feeder to inject or absorb vars as necessary to improve the voltage profile.

Faults on the distribution system may cause the line voltage to drop and trip the DG on low voltage. However, updated distribution grid codes issued by network operators require DGs to have the capability to withstand, or ride through, these voltage dips for a predefined time [4]. Therefore, following a fault, the voltage must recover quickly to a level above the protection trip setting. The response of OLTC or other conventional VR is slow [5], but the DGs themselves, in particular the inverter-interfaced DGs, can quickly supply the necessary vars to restore voltage and prevent the DG from tripping on low voltage [5]. Hence, the DGs must also participate in voltage control, especially following a fault or other emergency conditions.

With such a wide variety of voltage control equipment available on the distribution system, controlling the equipment becomes a challenge. Centralized and distributed methods have been proposed for the control of DG-integrated distribution systems [2]. Centralized methods include heuristic approaches, experts systems, and mathematical programming, while distributed methods are mainly based on multi-agent systems (MAS) [6]. The proposed solutions have the potential to improve the voltage performance of the distribution system. The major limitation of centralized methods is that these approaches depend on a central computer to perform the control function, leading to single point of failure. A distributed approach has advantages in this respect that failure of one node will only affect a localized portion of the distribution network [7]. To this end, distributed methods such as agent-based approaches have received significantly increased attention [6].

Several distributed methods based on the power flow sensitivity theory have been described. Research done in [8] proposes a MAS-based approach in which the power flow sensitivity coefficients are calculated at each node and a merit order is established that aims to optimize the total reactive power output from the DGs. The DG with highest sensitivity is dispatched first, and so on. The contract-net-protocol (CNP) [9] is used for agent interactions, where an agent experiencing low voltage at its node invites other agents with available reactive power capacity to contribute vars, according to the established merit order, until the required voltage boost is obtained. The work presented in [6] applies a similar concept but communication and request for support is limited to the two neighboring agents. In these methods, there is risk of conflict when more than one agent request var compensation at the same time, which may result in unpredictable compensations and possible "cycling" where the system fails to reach steady state condition.

The authors in [8–10] simplify the analysis by using $P\theta$-QV de-coupling which is typical for transmission but not accurate for distribution studies [11]. Other approaches, such as the ones given by [11], employ distributed control with local controllers at the feeder nodes that control var injection from local DG, but have an overall central controller that calculates the settings, leading to a hierarchical structure for the control algorithm.

The authors in [10] propose a MAS-based solution for optimal reactive power control (ORPC) using the subgradient method. ORPC concept aims at minimizing active power losses while improving the voltage profile. The ORPC is formulated as a constrained optimization problem. The reactive power control settings at the participating nodes are then adjusted according to the direction of the subgradients of the objective function, without solving the objective function itself. The algorithm, however, makes simplifying assumptions when solving the subgradients, that Q and P injections at a node affect only the voltage magnitude and voltage angle, respectively, at that node—voltages and their angles at all other nodes remaining fixed at their pre-existing values. This takes the simplification further than applying the $P\theta$-QV de-coupling model which, as already mentioned previously, is typical for transmission level analysis.

The solutions presented above consider that failure of communication for MAS-based control will only affect a localized portion of the distribution network and the issue is not discussed further. However, failure of the link even between the two neighboring nodes may have consequences for the entire feeder. As discussed later in Section 4 of this article, when an agent at a node is "blinded" through communication failure, this may affect the actions of agents elsewhere on the feeder.

Decentralized approaches that do not require any communications but depend only on local measurements have been proposed in the literature. These methods have the advantage of requiring no investment in communication systems. An early approach was curtailment of the active power output of the DG to manage the voltage profile [12]. Capacity curtailment, however, would result in loss of revenue to the DG owner. Some researchers propose, instead, the use of energy storage systems to manage the distribution system voltage profile. Work presented in [13] proposes decentralized storage achievable by integrating solar PV systems with local battery energy storage (BES). This strategy was shown to be effective with small PV systems of the order of kW, and with participation of every node with PV generation. This approach is also shown to be effective for systems with low X/R ratio where reactive power control alone has weaker impact on nodal voltages and may not be sufficient [13]. However, looking at the considerable costs of energy storage technology available today [14], this strategy may not be practical with DG of the order of megawatts (MW).

A major concern with decentralized control is the voltage instability that may result from interactions between the controllers of the multiple DG units on the network. To achieve stable voltage control, modeling is required to correctly capture the interactions among the DG units, resulting in very complex control algorithms. Where a linearized model is adopted, this must be corrected for any new system operating point. The authors in [12] presented the design of a multi-input multi-output (MIMO) decentralized controller requiring detailed models of the DG units and the distribution network. Attempt is made to ensure stability in the presence of model uncertainties. The algorithm manages to remove conflict between the controllers but significant changes to the DG and network configuration or characteristics may require extensive work to re-model the network.

The voltage control approach taken in this paper is distributed and uses MAS. The distribution feeder is split into a series of overlapping line segments, to each of which is allocated an agent. The agent senses the voltage variables in its segment and formulates reactive power compensation necessary to correct the voltage of that segment. The total coordinated actions of the agents eliminate any voltage deviations resulting from connection of DG or variation in loading conditions. The proposed solution removes the need for some assumptions, allowing the use of the non-decoupled load flow model to correctly capture the characteristics of the distribution feeder. Potential conflicts between the actions of the agents are resolved and impact of communication link failure reduced.

This article is organized as follows: Section 2 gives a detailed description of the formulation of the proposed algorithm for voltage control. The feasibility and performance of the proposed algorithm is demonstrated in Section 3. Section 4 discusses the simulation results and their implications. The conclusions are presented in Section 5.

2. PROPOSED VOLTAGE CONTROL ALGORITHM

The voltage at a node in a power network is a function of P and Q at that node, i.e., $V = f(P, Q)$. The load flow of a N-node power network can be expressed by the equations [15]:

$$\begin{cases} P_i = \sum_{j=1}^{N} V_i V_j Y_{ij} cos\left(\delta_i - \delta_j - \delta_{ij}\right) \\ Q_i = \sum_{j=1}^{N} V_i V_j Y_{ij} sin\left(\delta_i - \delta_j - \delta_{ij}\right) \end{cases} \quad (1)$$

where P_i and Q_i are the real and reactive power flow at node i; V_i and δ_i are, respectively, the voltage magnitude and angle at node i; V_j and δ_j are the voltage magnitude and angle at node j; Y_{ij} and δ_{ij} are, respectively, the magnitude and argument of the element (i, j) in the network's admittance matrix.

Changes in P and Q are related to changes in voltage by the partial differential equations [15]:

$$\begin{bmatrix} \Delta P \\ \Delta Q \end{bmatrix} = \begin{bmatrix} \frac{\partial P}{\partial \delta} & \frac{\partial P}{\partial V} \\ \frac{\partial Q}{\partial \delta} & \frac{\partial Q}{\partial V} \end{bmatrix} \cdot \begin{bmatrix} \Delta \delta \\ \Delta V \end{bmatrix} = \left[J_{PQ\delta V}\right] \cdot \begin{bmatrix} \Delta \delta \\ \Delta V \end{bmatrix} \quad (2)$$

$[J_{PQ\delta V}]$ is called the Jacobian matrix of the network. The elements of the Jacobian matrix give the sensitivity between power flow and bus voltage changes. Equation (2) gives the linearized model of the system around a given operating point and can be used to compute the expected small changes in δ and V for small changes in P and Q [16]. This type of sensitivity information is useful for estimating expected voltage changes which result from installation of reactive compensation. The Jacobian also provides useful information regarding voltage stability [16].

From Eq. (1), it can be noted that for a radial system,

$$Y_{ij} = 0\, if\ j < i - 1\ or\ j > i + 1 \quad (3)$$

This is depicted in Figure 1 for a 6-node radial network. Considering node 3 ($i = 3$), Y_{23} and Y_{34} have finite values, while Y_{13}, Y_{35}, and Y_{36} are equal to zero. The complete Y_{bus} matrix for this 6-node radial network is given by Eq. (4).

$$[Y_{bus}] = \begin{bmatrix} Y_{11} & Y_{12} & 0 & 0 & 0 & 0 \\ Y_{21} & Y_{22} & Y_{23} & 0 & 0 & 0 \\ 0 & Y_{32} & Y_{33} & Y_{34} & 0 & 0 \\ 0 & 0 & Y_{43} & Y_{44} & Y_{45} & 0 \\ 0 & 0 & 0 & Y_{54} & Y_{55} & Y_{56} \\ 0 & 0 & 0 & 0 & Y_{65} & Y_{66} \end{bmatrix} \quad (4)$$

The form of Y_{bus} implies that to obtain the power flow at node i, it is sufficient to consider only the voltages at the two adjacent nodes. Of course, the voltages at those adjacent nodes are influenced by voltages at their own adjacent nodes.

From Eq. (2), the changes in active power are given by,

$$[\Delta P] = \left[\frac{\partial P}{\partial \delta}\right][\Delta \delta] + \left[\frac{\partial P}{\partial V}\right][\Delta V] \quad (5)$$

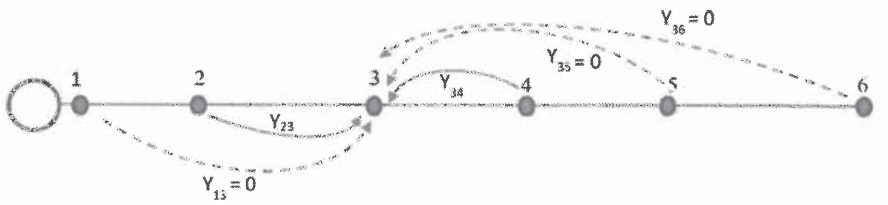

FIGURE 1. Six-node radial network.

And the changes in reactive power are given by,

$$[\Delta Q] = \left[\frac{\partial Q}{\partial \delta}\right][\Delta\delta] + \left[\frac{\partial Q}{\partial V}\right][\Delta V] \quad (6)$$

From Eq. (5), and for the 6-node radial network, the change in power at node 3 may be expressed as:

$$\Delta P_3 = \frac{\partial P_3}{\partial \delta_1}\Delta\delta_1 + \frac{\partial P_3}{\partial \delta_2}\Delta\delta_2 + \cdots + \frac{\partial P_3}{\partial \delta_6}\Delta\delta_6 + \frac{\partial P_3}{\partial V_1}\Delta V_1 + \frac{\partial P_3}{\partial V_2}\Delta V_2 + \cdots + \frac{\partial P_3}{\partial V_6}\Delta V_6 \quad (7)$$

However, according to Eqs. (3) and (4), only the terms within the band (–1 to +1) of the respective node (i) are of interest.

Hence, from Eqs. (1–3), for the 6-node radial network, the sub-matrix, $\frac{\partial P}{\partial \delta}$ can be written, thus:

$$\left[\frac{\partial P}{\partial \delta}\right] = \begin{bmatrix} \frac{\partial P_1}{\partial \delta_1} & \frac{\partial P_1}{\partial \delta_2} & 0 & 0 & 0 & 0 \\ \frac{\partial P_2}{\partial \delta_1} & \frac{\partial P_2}{\partial \delta_2} & \frac{\partial P_2}{\partial \delta_3} & 0 & 0 & 0 \\ 0 & \frac{\partial P_3}{\partial \delta_2} & \frac{\partial P_3}{\partial \delta_3} & \frac{\partial P_3}{\partial \delta_4} & 0 & 0 \\ 0 & 0 & \frac{\partial P_4}{\partial \delta_3} & \frac{\partial P_4}{\partial 4} & \frac{\partial P_4}{\partial \delta_5} & 0 \\ 0 & 0 & 0 & \frac{\partial P_5}{\partial \delta_4} & \frac{\partial P_5}{\partial \delta_5} & \frac{\partial P_5}{\partial \delta_6} \\ 0 & 0 & 0 & 0 & \frac{\partial P_6}{\partial \delta_5} & \frac{\partial P_6}{\partial \delta_6} \end{bmatrix} \quad (8)$$

Similar *tridiagonal* matrices can be written for $[\frac{\partial P}{\partial V}]$, $[\frac{\partial Q}{\partial \delta}]$, and $[\frac{\partial Q}{\partial V}]$. As can be seen from Eqs. (4) and (8), the sparsity of each sub-matrix of the Jacobian is the same as that of the node admittance matrix.

Equation (7) can, therefore, be re-written as:

$$\Delta P_3 = \frac{\partial P_3}{\partial \delta_2}\Delta\delta_2 + \frac{\partial P_3}{\partial \delta_3}\Delta\delta_3 + \frac{\partial P_3}{\partial \delta_4}\Delta\delta_4 + \frac{\partial P_3}{\partial V_2}\Delta V_2 + \frac{\partial P_3}{\partial V_3}\Delta V_3 + \frac{\partial P_3}{\partial V_4}\Delta V_4 \quad (9)$$

All the other terms of Eq. (7) are zeros. The equations for all nodes of the radial distribution network are of the form and size given by Eq. (9) irrespective of the number of nodes in the network.

Similiarly, from Eq. (6), the change in reactive power at node 3 may be expressed as:

$$\Delta Q_3 = \frac{\partial Q_3}{\partial \delta_2}\Delta\delta_2 + \frac{\partial Q_3}{\partial \delta_3}\Delta\delta_3 + \frac{\partial Q_3}{\partial \delta_4}\Delta\delta_4 + \frac{\partial Q_3}{\partial V_2}\Delta V_2 + \frac{\partial Q_3}{\partial V_3}\Delta V_3 + \frac{\partial Q_3}{\partial V_4}\Delta V_4 \quad (10)$$

Equations (8–10) show that changes at node 5, for example, do not *directly* impact the power flow at node 3. Changes at node 5 impact node 4; changes at node 4 impact node 3 in turn.

In general, Eq. (9) may be written as:

$$\Delta P_i = \frac{\partial P_i}{\partial \delta_{i-1}}\Delta\delta_{i-1} + \frac{\partial P_i}{\partial \delta_i}\Delta\delta_i + \frac{\partial P_i}{\partial \delta_{i+1}}\Delta\delta_{i+1} + \frac{\partial P_i}{\partial V_{i-1}}\Delta V_{i-1} + \frac{\partial P_i}{\partial V_i}\Delta V_i + \frac{\partial P_i}{\partial V_{i+1}}\Delta V_{i+1} \quad (11)$$

Similiarly, Eq. (10) may be written as:

$$\Delta Q_i = \frac{\partial Q_i}{\partial \delta_{i-1}}\Delta\delta_{i-1} + \frac{\partial Q_i}{\partial \delta_i}\Delta\delta_i + \frac{\partial Q_i}{\partial \delta_{i+1}}\Delta\delta_{i+1} + \frac{\partial Q_i}{\partial V_{i-1}}\Delta V_{i-1} + \frac{\partial Q_i}{\partial V_i}\Delta V_i + \frac{\partial Q_i}{\partial V_{i+1}}\Delta V_{i+1} \quad (12)$$

The terms $(\frac{\partial P_i}{\partial \delta_i}, \frac{\partial Q_i}{\partial \delta_i})$, $(\frac{\partial P_i}{\partial \delta_{i-1}}, \frac{\partial P_i}{\partial V_{i-1}}, \frac{\partial Q_i}{\partial \delta_{i-1}}, \frac{\partial Q_i}{\partial V_{i-1}})$ and $(\frac{\partial P_i}{\partial \delta_{i+1}}, \frac{\partial P_i}{\partial V_{i+1}}, \frac{\partial Q_i}{\partial \delta_{i+1}}, \frac{\partial Q_i}{\partial V_{i+1}})$ are the *sensitivity* coefficients for node i. These *coupling* terms describe the change in power (active and reactive) at one node caused by changes in the voltage at that node and at adjacent nodes. Conversely, the sensitivity coefficients describe the changes in voltage magnitudes and angles resulting from injection of power at a particular node, such as connection of a DG. For example, with reference to Figure 1, if a DG is brought on line at node 3 or its output is adjusted, the voltage at node 3 will change together with the voltages at the two adjacent nodes 2 and 4 by magnitudes dependent on the sensitivity coefficients of the nodes. The voltages at other distant nodes will change as well. This contrasts with the assumptions made in [1] that Q and P injections at a node affect only the voltage magnitude and voltage angle, respectively, at that node, as discussed in introduction section of this article.

From Eq. (12), the voltage angle variation at node i can be obtained as:

$$\Delta\delta_i = \left(\frac{\partial Q_i}{\partial \delta_i}\right)^{-1}\left[\Delta Q_i - \frac{\partial Q_i}{\partial \delta_{i-1}}\Delta\delta_{i-1} - \frac{\partial Q_i}{\partial \delta_{i+1}}\Delta\delta_{i+1} - \frac{\partial Q_i}{\partial V_{i-1}}\Delta V_{i-1} - \frac{\partial Q_i}{\partial V_i}\Delta V_i - \frac{\partial Q_i}{\partial V_{i+1}}\Delta V_{i+1}\right] \quad (13)$$

Substituting Eq. (13) into Eq. (11), gives:

$$\Delta V_i = \left[\left(\frac{\partial P_i}{\partial \delta_i}\right)^{-1}\left(\frac{\partial P_i}{\partial V_i}\right) - \left(\frac{\partial Q_i}{\partial \delta_i}\right)^{-1}\left(\frac{\partial Q_i}{\partial V_i}\right)\right]^{-1} \times \left(\left[\left(\frac{\partial P_i}{\partial \delta_i}\right)^{-1}\left[\Delta P_i - \frac{\partial P_i}{\partial \delta_{i-1}}\Delta\delta_{i-1} - \frac{\partial P_i}{\partial \delta_{i+1}}\Delta\delta_{i+1} - \frac{\partial P_i}{\partial V_{i-1}}\Delta V_{i-1} - \frac{\partial P_i}{\partial V_{i+1}}\Delta V_{i+1}\right]\right] - \left[\left(\frac{\partial Q_i}{\partial \delta_i}\right)^{-1}\left[\Delta Q_i - \frac{\partial Q_i}{\partial \delta_{i-1}}\Delta\delta_{i-1} - \frac{\partial Q_i}{\partial \delta_{i+1}}\Delta\delta_{i+1} - \frac{\partial Q_i}{\partial V_{i-1}}\Delta V_{i-1} - \frac{\partial Q_i}{\partial V_{i+1}}\Delta V_{i+1}\right]\right]\right) \quad (14)$$

Equation (14) gives the active and reactive compensation, ΔP_i and ΔQ_i, required to eliminate any voltage changes at a node resulting from connection of a DG, or any other cause. It can be seen from Eq. (14) that ΔV_i is zero if the following condition is satisfied:

$$\left(\frac{\partial P_i}{\partial \delta_i}\right)^{-1}\left[\Delta P_i - \frac{\partial P_i}{\partial \delta_{i-1}}\Delta\delta_{i-1} - \frac{\partial P_i}{\partial \delta_{i+1}}\Delta\delta_{i+1} - \frac{\partial P_i}{\partial V_{i-1}}\Delta V_{i-1} - \frac{\partial P_i}{\partial V_{i+1}}\Delta V_{i+1}\right] = \left(\frac{\partial Q_i}{\partial \delta_i}\right)^{-1}\left[\Delta Q_i - \frac{\partial Q_i}{\partial \delta_{i-1}}\Delta\delta_{i-1} - \frac{\partial Q_i}{\partial \delta_{i+1}}\Delta\delta_{i+1} - \frac{\partial Q_i}{\partial V_{i-1}}\Delta V_{i-1} - \frac{\partial Q_i}{\partial V_{i+1}}\Delta V_{i+1}\right] \quad (15)$$

Values of ΔP_i and ΔQ_i can be selected to make the two sides of Eq. (15) equal, effectively reducing Eq. (14), and hence, ΔV_i, to zero. These values of ΔP_i and ΔQ_i will depend on the sensitivity coefficient at the various nodes.

Of course, if a particular node has no capacity to inject power into the system, that node is not able to participate in voltage control. But the voltage drop at that node is noticed by adjacent nodes which, if they have generating capacity, will inject power to correct their respective voltage, in the process acting to support the voltage at the non-controlled adjacent node. This effect is apparent from Eqs. (11) and (12) where injection of power (active or reactive) at node i also affects the voltages at the adjacent nodes $(i-1)$ and $(i+1)$ by magnitudes dependent on the *transfer* sensitivities of those nodes.

Obviously it would not make sense to try and adjust the active power injection to control the voltage because this will give a trivial solution—for example, disconnect the DG and revert to the pre-existing system state, or generate reduced active power, which is not desirable. With the active power held constant, only the reactive power must be adjusted to mitigate voltage effects of connection of DG.

From Eq. (15), the reactive power compensation required is,

$$\Delta Q_i = \left(\frac{\partial Q_i}{\partial \delta_i}\right)\left(\frac{\partial P_i}{\partial \delta_i}\right)^{-1}\left[\Delta P_i - \frac{\partial P_i}{\partial \delta_{i-1}}\Delta\delta_{i-1} - \frac{\partial P_i}{\partial \delta_{i+1}}\Delta\delta_{i+1} - \frac{\partial P_i}{\partial V_{i-1}}\Delta V_{i-1} - \frac{\partial P_i}{\partial V_{i+1}}\Delta V_{i+1}\right] + \left[\frac{\partial Q_i}{\partial \delta_{i-1}}\Delta\delta_{i-1} + \frac{\partial Q_i}{\partial \delta_{i+1}}\Delta\delta_{i+1} + \frac{\partial Q_i}{\partial V_{i-1}}\Delta V_{i-1} + \frac{\partial Q_i}{\partial V_{i+1}}\Delta V_{i+1}\right] \quad (16)$$

This reactive power compensation will be adjusted until condition given by Eq. (15) is satisfied (with ΔP_i set to zero). It should be realized that other nodes with reactive power capability will also participate and inject reactive power of the correct sign, and of magnitude given by Eq. (16) at the respective node. So, beginning from a known state (node voltages), the system should be able to return to that original state if the DGs, or system, has sufficient reactive power capability.

Therefore, Eq. (16) provides the basis for control of the voltage profile of a radial distribution system. This algorithm is inherently distributed as only the two nodes adjacent to the control node are considered. This distributed algorithm is best implemented using the multi-agent concept, employing intelligent electronic devices (IEDs) and peer-to-peer communications.

The derivation above assumes that the system loads are voltage independent and will not change during the control period. This means that $\Delta P = \Delta Q = 0$ at all nodes except the nodes where DG is connected. Otherwise, the linearized load flow model of the system will not be static.

2.1. Multi-Agent Based Voltage Control

An agent is defined as an IED that is capable of autonomous action within an environment to meet its design objectives [17, 18]. The objective in this instance is the voltage control function. The "intelligent agent" has three main characteristics: reactive, proactive, and social abilities [8]. Reactiveness means ability of agent to recognize any changes in its environment and react with corresponding actions according to the goal of the agent. Pro-activeness depicts goal-based behaviors. The goal is objective of agent, which is set according to the system wide objective. The social ability of an intelligent agent is the ability to interact with other intelligent agents in its environment.

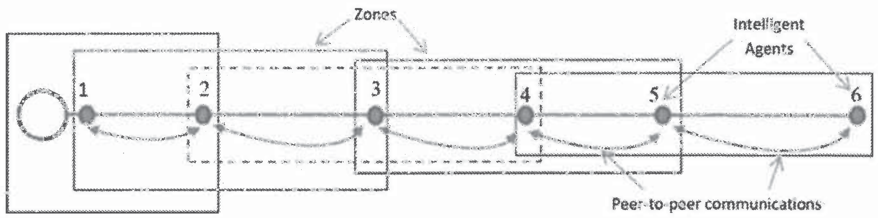

FIGURE 2. Multi-agent system for 6-node distribution system.

For the voltage control algorithm developed in this article, the IED agents are located at all the nodes on the distribution network such that the network is divided into multiple overlapping sections or zones, as depicted in Figure 2. The agents exchange data through peer-to-peer communications, essentially creating a network-wide, complex, distributed voltage control system. The proposed voltage control algorithm does not need centralized control, and will thus exhibit all the benefits and characteristics of distributed control: autonomy, flexibility, scalability, and robustness [8].

The *sensitivity* coefficients $(\frac{\partial P_i}{\partial \delta_i}, \frac{\partial Q_i}{\partial \delta_i})$, $(\frac{\partial P_i}{\partial \delta_{i-1}}, \frac{\partial P_i}{\partial V_{i-1}}, \frac{\partial Q_i}{\partial \delta_{i-1}}, \frac{\partial Q_i}{\partial V_{i-1}})$ and $(\frac{\partial P_i}{\partial \delta_{i+1}}, \frac{\partial P_i}{\partial V_{i+1}}, \frac{\partial Q_i}{\partial \delta_{i+1}}, \frac{\partial Q_i}{\partial V_{i+1}})$ at each node i are calculated in real-time and subsequently used for calculation of the required power injection at each node. The agents measure the voltage parameters (magnitude and angle) at the node at which they are located, sharing this information with the two adjacent agents, as illustrated in Figure 2.

However, the voltage angle, δ, is not an absolute quantity and cannot be measured by the local agent. The important quantity, in this instance, is the phase shift $(\delta_i - \delta_{i\pm 1})$ between the voltages at the two neighboring nodes. This can be determined if the zero crossing time instants of the two voltages at the two nodes are known. The agent should, therefore, in addition to measuring the voltage magnitude, also measure the time instant of zero crossing of the voltage, and make this information available to the two neighboring agents. The phase shift angle can then be calculated. The time stamps of all the agents on the feeder must be synchronized.

2.2. Determination of the Sensitivity Coefficients

The sensitivity coefficients can be determined from Eq. (2) which is derived from the power flow Eq. (1). From Eqs. (3) and (4) it was determined that, for the radial system, the elements Y_{ij} are zero if $j < i - 1 or j > i + 1$. This realization greatly simplifies the analysis of the voltage problem as only three nodes are relevant for the calculation of power flow at any node of the radial system. The radial distribution line can be assumed to be made up of overlapping sections (see Figure 2), with each section modelled as shown in Figure 3.

The power flow at any node i of the distribution system is, thus, given by:

$$\begin{cases} P_i = V_i V_{i-1} Y_{i(i-1)} \cos\left(\delta_i - \delta_{i-1} - \delta_{i(i-1)}\right) \\ \quad + V_i V_i Y_{ii} \cos\left(-\delta_{ii}\right) + V_i V_{i+1} Y_{i(i+1)} \cos \\ \quad \left(\delta_i - \delta_{i+1} - \delta_{i(i+1)}\right) \\ Q_i = V_i V_{i-1} Y_{i(i-1)} \sin\left(\delta_i - \delta_{i-1} - \delta_{i(i-1)}\right) \\ \quad + V_i V_i Y_{ii} \sin\left(-\delta_{ii}\right) + V_i V_{i+1} Y_{i(i+1)} \sin \\ \quad \left(\delta_i - \delta_{i+1} - \delta_{i(i+1)}\right) \end{cases} \tag{17}$$

The *sensitivity* coefficients can be directly and easily derived from Eq. (17), and these are given in the Appendix.

2.3. MAS-Based Reactive Power Dispatch

The central issue in MAS-based approach is how the agents cooperate and coordinate their actions [9]. This is usually achieved by constructing a plan that specifies all actions the agents need to take in order to achieve the overall goal.

The algorithm proposed in this article calculates the compensation required at each node for a specific voltage profile. The calculated compensations are, therefore, not mutually exclusive, for example, they cannot be applied simultaneously. Compensation at one node will affect the voltages at all the other nodes. Hence, only one of these should be applied at a time. A new voltage profile is then created that generates a new set of compensations at the various nodes. The dispatch of the calculated mega-var (MVAr) compensation is, therefore, an important issue to ensure the minimum vars are deployed to eliminate the voltage errors. The agents in the multiple line segments thus need to cooperate in their actions.

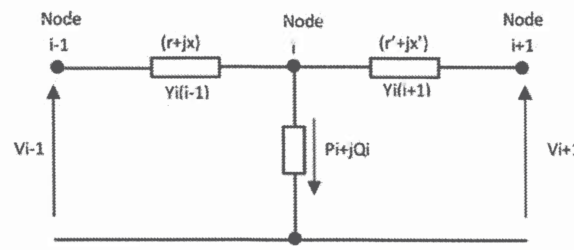

FIGURE 3. Radial distribution line segment.

Criteria for allocation of the var injection between the multiple DGs and other equipment located at the various nodes that are capable of participating in voltage control needs to be developed. A possible criterion is based on the Q-V sensitivity element, derived from Eq. (17) as,

$$\frac{\partial Q_i}{\partial V_i} = V_{i-1} Y_{i(i-1)} \sin\left(\delta_i - \delta_{i-1} - \delta_{i(i-1)}\right) + 2V_i Y_{ii} \sin(-\delta_{ii}) + V_{i+1} Y_{i(i+1)} \sin\left(\delta_i - \delta_{i+1} - \delta_{i(i+1)}\right) \quad (18)$$

This sensitivity element has an important implication. If $\frac{\partial Q_i}{\partial V_i}$ is small, a smaller amount of vars is required for a given change in voltage. In order to minimize the var requirement, this element can be used to identify the node, and the corresponding vars, to be injected. The calculation of the sensitivity coefficients is distributed, with each agent calculating the Q-V sensitivity at its node. The calculated values need to be made available to all the other agents on the feeder through peer-to-peer communications. No central computer is required for this purpose.

Emerging protocols such as the IEC61850 are capable of transmitting critical data through generic object oriented substation event (GOOSE) and sampled values (SV) messaging mechanisms [19]. Under this protocol, the agents (IEDs) use multi-cast transmission to broadcast GOOSE messages containing the measured values onto the communication network for use by other devices. Transmission of current and voltage values over IEC61850 protocol has been investigated in [20] for possible application of the protocol on the distribution system, outside of the substation for which it was initially intended. In fact, despite the fact the first IEC61850 release (of 2003) was conceived to cover substation automation only, edition 2 (of 2011) was broadened and covers now "Communication Networks and Systems in Power Utility Automation" which extends application to the MV network [20, 21].

The implementation of the MAS-based algorithm is, thus, as follows:

1. The first set of calculations is performed to generate a set of compensations for each of the nodes.
2. The node with the least $\frac{\partial Q_i}{\partial V_i}$ sensitivity is identified.
3. The corresponding compensation is injected at this node.
4. The resulting voltage changes generate a new operating point and the magnitudes of the sensitivity coefficients are affected (see the Appendix) such that the condition given by Eq. (14) is offset or is disturbed from its equilibrium point, and a further voltage deviation will appear. An additional compensation is, therefore, required to remove this offset. Hence, a second calculation, or iteration, is performed to give the additional compensation that must be added to the previously calculated value.
5. The node with the least $\frac{\partial Q_i}{\partial V_i}$ from this second calculation is identified and the vars injected.
6. A third calculation is performed, etc., if necessary, until changes in ΔQ_i from one iteration to the next are so small as be considered insignificant.

3. SIMULATION RESULTS

The 6-node network represented in Figure 4 was implemented in Digsilent *Powerfactory* software. The system parameters are given in Tables 1–4. The load is uniformly distributed along the feeder. The base case voltage profile is shown in Figure 5. This base case is given at low load conditions, which is the condition under which the voltage increase is highest when DG is connected [11, 22]. The automatic voltage regulator (AVR) at the feeder substation is set to maintain the transformer LV, or node 1, voltage at 1.04 p.u. As can be seen from Figure 5, the voltages at all nodes are within the acceptable range of 0.95 to 1.05 p.u. for this base case.

Maintaining the transformer LV voltage at a constant voltage is important as this decouples the MV feeders where more than one feeder are being fed from the same transformer. The result is that each feeder operates without the influence of the other lines. That is, the loads and generators connected to other feeders do not influence the voltage profile of the line considered. The results in this article show that the transformer LV (node 1) voltage did drop by a maximum 0.23%, as noted later in this section. This can be attributed to tolerances or limitations of the AVR.

A small wind farm with three 2.3 MW wind generators is connected at each node in turn. The generators are set to operate at unity power factor. The resulting voltage profiles, at

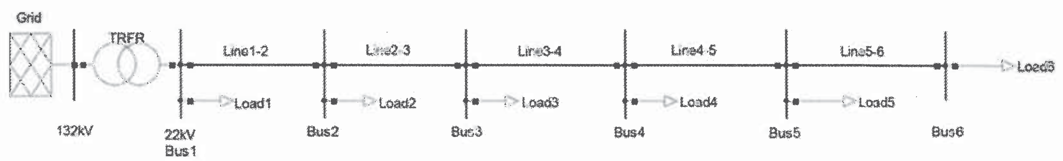

FIGURE 4. The 6-node network considered in the simulation.

MV voltage/kV	X-sectional area/mm^2	R1 Ω(/km)	X1 Ω(/km)	B (S/km)	Rating (Amps)
22	122.48	0.193	0.309	3.751	292

TABLE 1. Line parameters

MV Line1-2	MV Line2-3	MV Line3-4	MV Line4-5	MV Line5-6
5	5	5	5	5

TABLE 2. Line lengths (km)

HV	LV	Rating	Reactance
132 kV	22 kV	40 MVA	3%

TABLE 3. Transformer parameters

Load	S/MVA	CosΦ
Load1	2	0.95
Load2	2	0.95
Load3	2	0.95
Load4	2	0.95
Load5	2	0.95
Load6	2	0.95

TABLE 4. Load characteristics

minimum load conditions, are shown in Figure 5. It can be seen that the worst voltage excursion occurs with the DG connected at node 6, with the voltage rising to 1.069 p.u., which is outside the acceptable voltage limits.

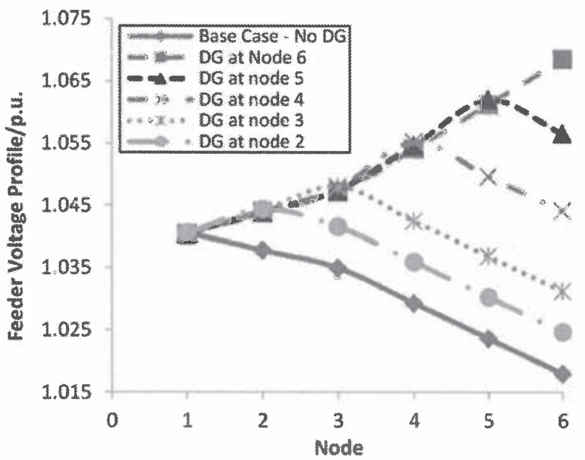

FIGURE 5. Feeder voltage profile with DG connected at each node in turn (under low load conditions).

Node	ΔQ_i [MVAr]		$\frac{\partial Q_i}{\partial V_i}$ [p.u.]	
	1st iteration	2nd iteration	1st iteration	2nd iteration
1	0.0959	1.2286	−4.6061	−4.5962
2	−1.9348	0.5389	−2.3016	−2.2715
3	−2.9685	0.1567	−1.7054	−1.6640
4	−4.0514	−0.2806	−1.1097	−1.0565
5	−6.2081	−0.7695	−1.0831	−1.0038
6	−3.1143	−0.4080	−1.0602	−0.9696

TABLE 5. Accumulative reactive compensation calculated values (with DG at node 6)

The proposed algorithm is tested in the first case with DG connected at node 6. The changes in voltage and angle at all nodes are monitored. These changes are substituted into Eq. (16) to determine the reactive power compensation required to eliminate the voltage change. The required compensation is calculated for each node and the results are shown in Table 5. It should be noted, as already discussed in Section 2.3, that these are not mutually exclusive compensations, for example, they cannot be applied simultaneously. Compensation at one node will affect the voltages at all the other nodes. Hence, only one of these should be applied at a time, and any further compensation re-calculated.

The voltage profiles resulting from applying the calculated compensations, independently, at each node are shown in Figure 6. As can be seen, compensation at node 6, where the DG is connected, generates voltage profile closest to the base case. It can also be seen from Table 5 that node 6 has the lowest value for $\frac{\partial Q_i}{\partial V_i}$ for this case. The negative values of the $\frac{\partial Q_i}{\partial V_i}$ elements imply that if the voltage is high, reactive power must be reduced or absorbed from the network.

The first set of calculations, therefore, requires that −3.1143 MVAr be injected at node 6 to lower the voltage. The voltage profile resulting from this compensation is shown in Figure 7. This voltage profile is offset from the base case profile. An additional compensation is therefore required to remove this offset. A second calculation, or iteration, is performed to give the additional compensation (−0.4080 MVAr) to be added to the previously calculated value. Additional calculations up to the sixth iteration are performed for this case. This accumulative generation of the compensation is described by Figure 8.

It is seen from Figure 8 that the initial calculations generate large values, and these values reduce in magnitude for subsequent iterations until the required compensation levels out. The calculation in this case effectively converges after the third iteration. The fourth to sixth iterations give little additional vars. full compensation (−3.5799 MVAr) at node 6

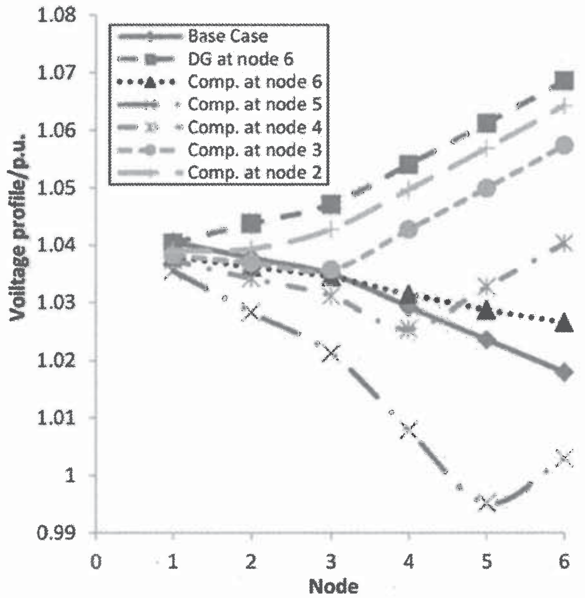

FIGURE 6. Feeder voltage profile with reactive power compensation at each of the nodes (under low load conditions) with DG connected at node 6.

leaves a 0.196% error in the node 6 voltage compared to the base case value. It can also be noted from Figure 7 that the voltage at the transformer LV (node 1) dropped by 0.23% in spite of the AVR control at that node.

As can be seen from Table 5, following the initial compensation of –3.1143 MVAr at node 6, there is drastic reduction in the var requirements at all the other nodes. For example, –6.2081 MVAr would have been required at node 5, but this drops to only –0.7695 MVAr. This realization emphasises the

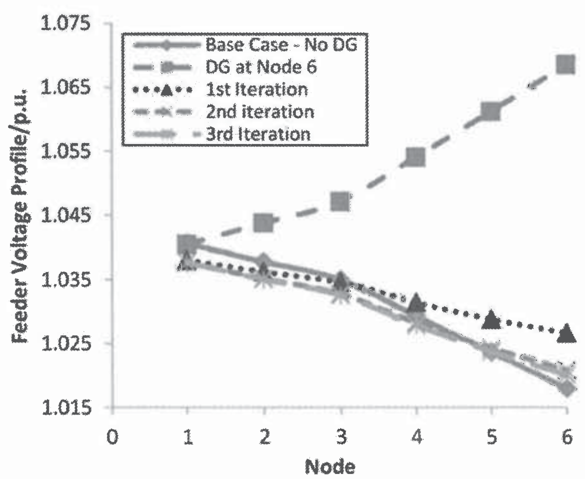

FIGURE 7. Feeder voltage profile with accumulative reactive power compensation at node 6 (under low load conditions).

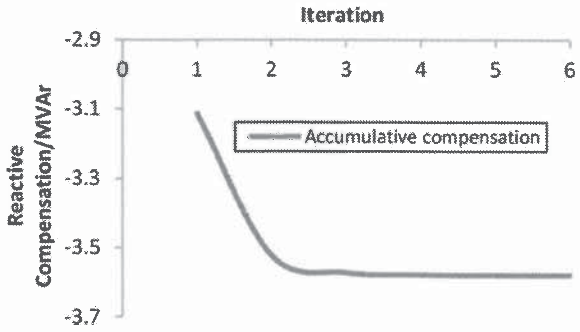

FIGURE 8. Accumulative reactive power compensation to restore node voltage.

fact that these var requirements are not mutually exclusive and should not be applied simultaneously.

Table 6 and Figure 9 show compensation results for the second case with DG connected at node 4. As can be seen from the figure, compensation at node 4 gives, at the first iteration, a voltage profile that best approximates the base case. It can also be seen from Table 6 that node 4 has the lowest value for $\frac{\partial Q_i}{\partial V_i}$ for the first iteration in this case. The second iteration identifies node 5 (lowest $\frac{\partial Q_i}{\partial V_i}$) as the one at which vars should be injected (absorbed).

Figure 10 shows the results of the accumulative var injection to restore voltage profile for this case with the DG connected at node 4. The first injection is for –3.1694 MVar at node 4; the second is for –0.5973 MVAr at node 5. The third and fourth iterations further required injection of vars at node 5.

4. DISCUSSION

Voltage control requires the reduction or absorption of reactive power at a node in case of high voltage, or injection of positive vars if the voltage is low. The DG itself can supply the required reactive power. However, where the DG is not capable of supplying, or absorbing, the required vars, external equipment should be connected such as static voltage com-

	ΔQ_i [MVAr]		$\frac{\partial Q_i}{\partial V_i}$ [p.u.]	
Node	1st iteration	2nd iteration	1st iteration	2nd iteration
1	0.0568	1.1757	–4.6060	–4.5958
2	–2.0428	0.38325	–2.3021	–2.2720
3	–3.1114	–0.0494	–1.7062	–1.6648
4	–3.1694	–0.3096	–1.1109	–1.0654
5	–4.2684	–0.5973	–1.1145	–1.0617
6	–2.1288	–0.2979	–1.1212	–1.0688

TABLE 6. Accumulative reactive compensation calculated values (with DG at node 4)

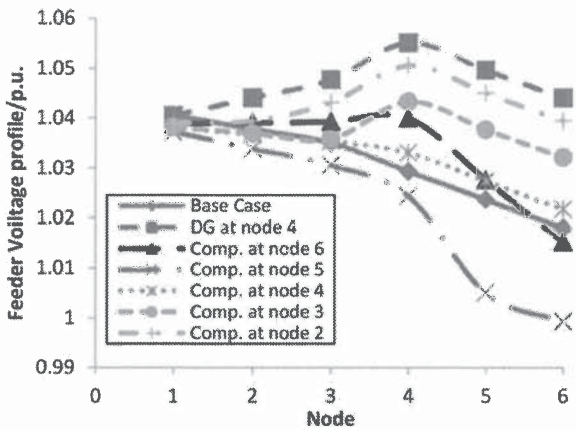

FIGURE 9. Feeder voltage profile with reactive power compensation at each of the nodes (under low load conditions) with DG connected at node 4.

pensators (SVCs) or static compensators (STATCOM). Initial studies can be performed during the planning stage of the DG integration to evaluate its impact on the voltage profile and see how much support is required when specific DG is integrated. This study should take into consideration the capabilities of already existing DGs and other voltage control equipment. It is important that the system be able to supply the required var compensation.

The proposed algorithm is simple and effective and minimizes the total var requirement to eliminate any voltage vari-

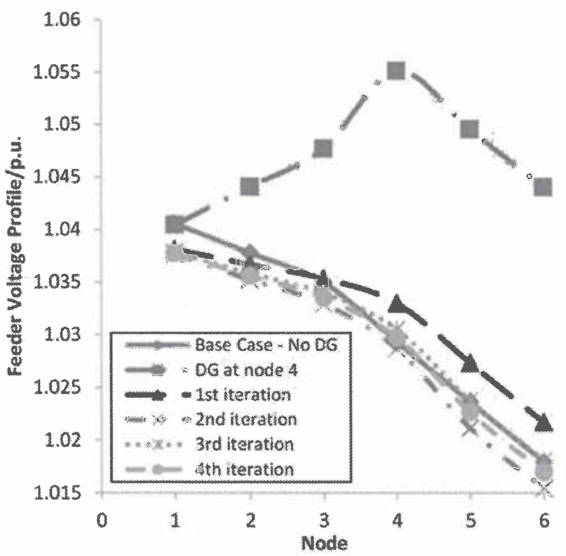

FIGURE 10. Feeder voltage profile with accumulative reactive power compensation with DG connected at node 4 (under low load conditions).

ations from the pre-planned base case. The algorithm is independent of feeder characteristics—whether overhead line (OHL) or cable, weak or stiff system. It can be applied to any distribution system that consists of radial feeders.

The simplicity of the algorithm results from the fact that the distributed algorithm depends only on local measurements and minimal communication with the two adjacent nodes. No huge communication loads associated with a central computer are involved.

However, a break in communication between any two agents will cause the community of agents on the distribution feeder to be effectively split into two groups. Information about the Q-V sensitivities at all nodes will now not be available to nodes in the separated group. The two groups will then attempt to independently try and adjust the node voltages in their section of the feeder. Voltage changes in one section will impact voltages on the other section, leading to a conflict situation. The voltage measurements will then be in a continuous state of flux and the controller calculations cannot give steady outputs. A steady state voltage may not be achieved. A possible resolution to this is for the agents to retain and use the last set of Q-V sensitivity values stored in memory before communication is lost. Any vars, if required, will be dispatched according to this last known Q-V sensitivity order, removing the conflict situation and, hence, improve the robustness of the algorithm against communication link failure.

The contribution of this article is the introduction of the concept of modeling the distribution feeder as a series of overlapping segments to facilitate distributed monitoring and control. This structure simplifies the analysis and solution of the distribution problem in that only three nodes need to be considered irrespective of the size (total number of nodes) of the distribution feeder. In this article, this allowed use of the non-decoupled load flow model which accurately represents the characteristics of the distribution feeder with low X/R ratio. No assumptions are necessary that lead to use of the simplified decoupled model, which is typically for transmission load flow studies. A MAS-based algorithm is then developed based on this line structure that is capable of eliminating any voltage deviation at any node on the feeder, through the coordinated actions of the agents located in the line segments.

5. CONCLUSION

The integration of DG in distribution networks has increased the complexity of the voltage control problem rendering traditional control methods ineffective. The voltage control algorithm proposed in this article, based on MAS and sensitivity theory, eliminates any voltage deviation resulting from connection of DG. The distributed control is realized through modeling the distribution feeder as a series of overlapping segments. The coordinated reactive compensation control actions of the agents located in the various line segments eliminate any voltage deviations, restoring the feeder voltage profile to the pre-planned base case profile. The main advantage of the proposed approach is that the agents can solve the voltage problem without the intervention of any central controller and by communication only between neighboring agents. The algorithm removes any potential for conflict between the control actions of the agents, and the impact of communication link failure is reduced improving the robustness of the control method.

In future work, the impact of the proposed algorithm on active power loss in the system will be investigated; optimal voltage control should be achieved at minimal power loss. In the smart grid, vars at a node can be provided by one or more of SVC, STATCOM, and DG. A procedure for coordinated allocation of the vars at that node needs to be developed. Finally, the sensitivity coefficients need to be determined experimentally by the agents for the algorithm to be system model independent.

REFERENCES

[1] Roy, N. K., and Pota, H. R., "Current status and issues of concern for the integration of distributed generation into electricity networks," *IEEE Syst. Journal*, Vol. 9, No. 3, pp. 933–944, February 2014.

[2] Carvalho, P. M. S., Correia, P. F., and Ferreira, L. A. F., "Distributed reactive power generation control for voltage rise mitigation in distribution networks," *IEEE Trans. Power Syst.*, Vol. 23, No. 2, pp. 766–772, May 2008.

[3] Chaitusaney, S., and Yokoyama, A., "Influence and prevention of voltage violation and momentary electricity interruption resulting from renewable energy sources," in *Proceedings of the IEEE Power Tech Conference*, Lausanne, France, pp. 437–442, 1–5 July 2007.

[4] Eissa, M. M., "Protection techniques with renewable resources and smart grids—A survey," *Renew. Sustain. Energy Rev.*, Vol. 52, pp. 1645–1667, December 2015.

[5] He, Y., Petit, M., and Dessante, P., "Optimization of the steady voltage profile in distribution systems by coordinating the controls of distributed generations," in *Proceedings of the 3rd IEEE PES Innovative Smart Grid Technologies Conference (ISGT Europe)*, Berlin, Germany, pp. 1–7, 14–17 October 2012.

[6] Chen, X., Zhang, C., Zhang, W., and Zhou, J., "Study of multi-agent based distributed control for distribution system with integration of distributed generations," in *Proceedings of the 8th International Power Engineering and Optimization Conference (PEOCO2014)*, Langkawi, Malaysia, pp. 220–224, 24–25 March 2014.

[7] Manditereza, P. T., and Bansal, R. C., "Renewable distributed generation: The hidden challenges—A review from the protection perspective," *Renew. Sustain. Energy Rev.*, Vol. 58, pp. 1457–1465, May 2016.

[8] Ahmad, I., Palensky, P., and Gawlik, W., "Multi-agent system based voltage support by distributed generation in smart distribution network," in *Proceedings of the IEEE International Symposium on Smart Electric Distribution Systems and Technologies (EDST)*, pp. 329–334, Vienna, Austria, 8–11 September 2015.

[9] Baran, M. E., and El-Markabi, I. M., "A multiagent-based dispatching scheme for distributed generators for voltage support on distribution feeders," *IEEE Trans. Power Syst.*, Vol. 22, No. 1, pp. 52–59, February 2007.

[10] Zhang, W., Liu, W., Wang, X., Liu, L., and Ferrese, F., "Distributed multiple agent system based online optimal reactive power control for smart grids," *IEEE Trans. Smart Grid*, Vol. 5, No. 5, pp. 2421–2431, September 2014.

[11] Brenna, M., De Berardinis, E., Delli Carpini, L., Foiadelli, F., Paulon, P., Petroni, P., Sapienza, G., Scrosati, G., and Zaninelli, D., "Automatic distributed voltage control algorithm in smart grids applications," *IEEE Trans. Smart Grid*, Vol. 4, No. 2, pp. 877–885, June 2013.

[12] Di Fazio, A. R., Fusco, G., and Russo, M., "Decentralized voltage control of distributed generation using a distribution system structural MIMO model," *Control Engineer. Practice* (article in press accepted December 2015), http://dx.doi.org/10.1016/j.conengprac.2015.12.016i.

[13] Kabir, M. N., Mishra, Y., Ledwich, G., Xu, Z., and Bansal, R. C., "Improving voltage profile of residential distribution systems using rooftop PVs and battery energy storage systems," *Appl. Energy, Vol.*. 134, pp. 290–300, August 2014.

[14] Madani, V., Das, R., Aminifar, F., McDonald, J., Venkata, S. S., Novosel, D., Bose, A., and Shahidehpour, M., "Distribution automation strategies challenges and opportunities in a changing landscape," *IEEE Trans. Smart Grid*, Vol. 6, No. 4, pp. 2157–2165, July 2015.

[15] Weedy, B. M., Cory, B. J., Jenkins, N., Ekanayake, J. B., and Strbac, G., *Electric Power Systems*, 5th ed, Chichester, West Sussex, England: John Wiley, 2012.

[16] Kundur, P., *Power System Stability and Control*, N. J. Balu and M. G. Lauby (Eds.), New York: McGraw-Hill, 1994.

[17] Wan, H., Wong, K. P., and Chung, C.,Y., "Multi-agent application in protection coordination of power system with distributed generations," in *Proceedings of the IEEE Power and Energy Society General Meeting—Conversion and Delivery of Electrical Energy in the 21st Century*, pp. 1–6, Pittsburgh, PA, 20–24 July 2008.

[18] Yorino, N., Zoka, Y., Watanabe, M., and Kurushima, T., "An optimal autonomous decentralized control method for voltage control devices by using a multi-agent system," *IEEE Trans. Power Syst.*, Vol. 30, No. 5, pp. 2225–2233, September 2015.

[19] Das, R., Madani, V., Aminifar, F., McDonald, J. S. Venkata, S., Novosel, D., Bose, A., and Shahidehpour, M., "Distribution automation strategies: Evolution of technologies and the business case," *IEEE Trans. Smart Grid*, Vol. 6, No. 4, pp. 2166–2175, July 2015.

[20] Giustina, D. D., Dede, A., De Sotomayor, A. A., and Ramos, F., "Toward an adaptive protection system for the distribution grid by using the IEC 61850," in *Proceedings of the IEEE International Conference on Industrial Technology (ICIT)*, Seville, Spain, pp. 2374–2378, 17–19 March 2015.

[21] Dawidczak, H., Dufaure, T., and Englert, H., "Compatibility of IEC61850 Edition 1 and Edition 2 Implementations," in *Proceedings of the CIRED 21st International Conference on*

Electricity Distribution, Frankfurt, Germany, pp. 1–4, 6–9 June 2011.

[22] Mahmud, M. A., Hossain, M. J., and Pota, H. R., "Voltage variation on distribution networks with distributed generation: Worst case scenario," *IEEE Syst. Journal*, Vol. 8, No. 4, pp. 1096–1103, December 2014.

APPENDIX

The sensitivity coefficients for the node i of the three-node line segment are given by:

$$\begin{cases} \frac{\partial P_i}{\partial \delta_i} = -V_i V_{i-1} Y_{i(i-1)} \sin\left(\delta_i - \delta_{i-1} - \delta_{i(i-1)}\right) \\ \quad - V_i V_{i+1} Y_{i(i+1)} \sin\left(\delta_i - \delta_{i+1} - \delta_{i(i+1)}\right) \\ \frac{\partial Q_i}{\partial \delta_i} = V_i V_{i-1} Y_{i(i-1)} \cos\left(\delta_i - \delta_{i-1} - \delta_{i(i-1)}\right) \\ \quad + V_i V_{i+1} Y_{i(i+1)} \cos\left(\delta_i - \delta_{i+1} - \delta_{i(i+1)}\right) \\ \frac{\partial P_i}{\partial \delta_j} = V_i V_j Y_{ij} sin\left(\delta_i - \delta_j - \delta_{ij}\right) \\ \frac{\partial P_i}{\partial V_j} = V_i Y_{ij} cos\left(\delta_i - \delta_j - \delta_{ij}\right) \\ \frac{\partial Q_i}{\partial \delta_j} = -V_i V_j Y_{ij} cos\left(\delta_i - \delta_j - \delta_{ij}\right) \\ \frac{\partial Q_i}{\partial V_j} = V_i Y_{ij} sin\left(\delta_i - \delta_j - \delta_{ij}\right) \end{cases}$$

where $j = (i-1)\, or\, (i+1)$, respectively, for the two nodes adjacent to node i.

BIOGRAPHIES

Patrick T. Manditereza received his B.Sc. in electrical engineering from the University of Zimbabwe in 1991 and his M.Sc. from the University of Bradford, United Kingdom, in 1997. He joined the Zimbabwe Electricity Supply Authority as protection engineer in 1991. In 1996 he joined the National University of Science and Technology, Zimbabwe, as lecturer and also consulted widely with the mining and electrical industries. He moved to the Polytechnic of Namibia, Windhoek, in 2004. Since 2006 he has been with the Central University of Technology, Free State, South Africa. He is also currently pursuing his Ph.D. studies with the University of Pretoria, South Africa. He is registered Professional Engineer (Pr Eng) with the Engineering Council of South Africa (ECSA).His research interests include the integration of renewable energy resources, protection of DG integrated networks, smart grids and micro-grids, and low voltage dc (LVDC) power distribution.

Ramesh C. Bansal has more than 25 years of teaching, research, and industrial experience. Currently, he is the Professor and Group head (Power) in the Department of Electrical, Electronic and Computer Engineering at University of Pretoria, South Africa. In previous postings he was with the University of Queensland, Australia, Birla Institute of Technology and Science, Pilani, India; the University of the South Pacific, Fiji; and Civil Construction Wing, All India Radio. He has published over 240 articles in journals and conferences. Professor Bansal is an Editor/Associate Editor of many reputed journals including IET-Renewable Power Generation and Electric Power Components and Systems. He is a Fellow, and CP Engg IET-UK, Fellow Engineers Australia, Fellow Institution of Engineers (India) and Senior Member-IEEE. He has diversified research interests in the areas of Renewable Energy and Conventional Power Systems which includes wind, PV, hybrid power systems, distributed generation, grid integration of renewable energy, power systems analysis (reactive power/voltage control, stability, faults, and protection), smart grid, FACTS and power quality.